Maternal high fat–high energy diet alters metabolic factors in the non-human primate fetal heart

Melanie R. Bertossa[1] , Jack R. T. Darby[1] , Stacey L. Holman[1] , Ashley S. Meakin[1] , Cun Li[2], Hillary F. Huber[3] , Michael D. Wiese[4] , Peter W. Nathanielsz[2] and Janna L. Morrison[1]

[1] *Early Origins of Adult Health Research Group, Health and Biomedical Innovation, University of South Australia, Adelaide, South Australia, Australia*
[2] *Department of Animal Science, University of Wyoming, Laramie, WY, USA*
[3] *Southwest National Primate Research Center, Texas Biomedical Research Institute, San Antonio, TX, USA*
[4] *Centre for Pharmaceutical Innovation, UniSA: Clinical and Health Sciences, University of South Australia, Adelaide, South Australia, Australia*

Handling Editors: Laura Bennet & Kyle McCommis

The peer review history is available in the Supporting Information section of this article (https://doi.org/10.1113/JP286861#support-information-section).

The Journal of Physiology
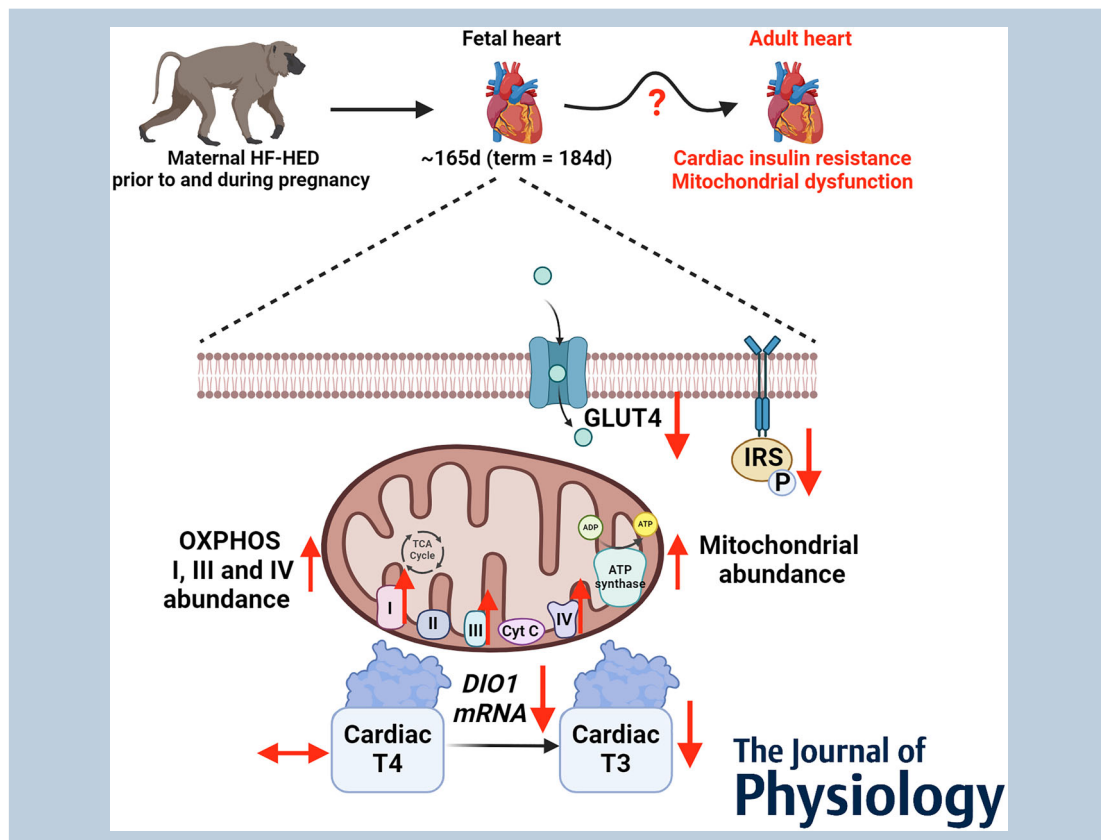
Melanie Bertossa received her Bachelor of Medical Science at the University of South Australia. She is pursuing a PhD at the University of South Australia in the Early Origins of Adult Health Research Group under the supervision of Professor Janna Morrison, Dr. Jack Darby, and Associate Professor Michael Wiese. Her research interests are maternal nutrition during pregnancy, fetal development and lifelong health.
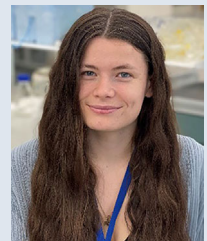
Abstract The consumption of high fat–high energy diets (HF-HEDs) continues to rise worldwide and parallels the rise in maternal obesity (MO) that predisposes offspring to cardiometabolic disorders. Although the underlying mechanisms are unclear, thyroid hormones (TH) modulate cardiac maturation *in utero*. Therefore, we aimed to determine the impact of a high fat–high energy diet (HF-HED) on the hormonal, metabolic and contractility profile of the non-human primate (NHP) fetal heart. At ∼9 months preconception, female baboons (*Papio hamadryas*) were randomly assigned to either a control diet or HF-HED. At 165 days gestational age (term = 184 days), fetuses were delivered by Caesarean section under anaesthesia, humanely killed, and left ventricular cardiac tissue (Control (n = 6 female, 6 male); HF-HED (n = 6 F, 6 M)) was collected. Maternal HF-HED decreased the concentration of active cardiac TH (i.e. triiodothyronine (T3)), and type 1 iodothyronine deiodinase (*DIO1*) mRNA expression. Maternal HF-HED decreased the abundance of cardiac markers of insulin-mediated glucose uptake phosphorylated insulin receptor substrate 1 (Ser789) and glucose transporter 4, and increased protein abundance of key oxidative phosphorylation complexes (I, III, IV) and mitochondrial abundance in both sexes. Maternal HF-HED alters cardiac TH status, which may induce early signs of cardiac insulin resistance. This may increase the risk of cardiometabolic disorders in later life in offspring born to these pregnancies.

Abstract figure legend Maternal high fat–high energy diet (HF-HED) prior to and throughout pregnancy alters the fetal cardiometabolic profile. This includes decreased markers of insulin-dependent glucose uptake, increased mitochondrial abundance, and oxidative phosphorylation (OXPHOS) complex I, III and IV. Maternal HF-HED decreased fetal cardiac thyroid hormone triiodothyronine (T3) concentrations and type 1 iodothyronine deiodinase (*DIO1*) mRNA expression. Maternal HF-HED may increase the risk of cardiometabolic disorders in the adult heart.

Key points

- Babies born to mothers who consume a high fat–high energy diet (HF-HED) prior to and during pregnancy are predisposed to an increased risk of cardiometabolic disorders across the life course.
- Maternal HF-HED prior to and during pregnancy decreased thyroid hormone triiodothyronine (T3) concentrations and type 1 iodothyronine deiodinase *DIO1* mRNA expression in the non-human primate fetal heart.
- Maternal HF-HED decreased markers of insulin-dependent glucose uptake, phosphorylated insulin receptor substrate 1 and glucose transporter 4 in the fetal heart.
- Maternal HF-HED increased mitochondrial abundance and mitochondrial OXPHOS complex I, III and IV in the fetal heart.
- Fetuses from HF-HED pregnancies are predisposed to cardiometabolic disorders that may be mediated by changes in T3, placing them on a poor lifetime cardiovascular health trajectory.

Introduction

The popularity and availability of a Western-style diet, high in fructose and rich in saturated and trans-fatty acids, is increasing (Rakhra et al., 2020). This increase in high-fat diet (HFD) consumption is a major contributing factor to the prevalence of obesity, which has almost tripled since 1975 such that more than 650 million people worldwide were obese in 2016 (World Health Organization, 2021).

Concerningly, women of childbearing age are now more likely to enter pregnancy with HFDs and obesity (Wang et al., 2021).

Babies born to mothers with obesity (maternal obesity, MO) and HFDs during pregnancy are often large for gestational age and predisposed to an increased risk of cardiometabolic disorders across the life course (Lee et al., 2015; McMillen et al., 2009; Zambrano

& Nathanielsz, 2013). Specifically, offspring from pregnancies complicated with MO have a 16% increase in pathological cardiovascular events before the age of 25 as well as a 30% increase in the risk of hospital admission for a cardiovascular event in adulthood (Lee et al., 2015; Razaz et al., 2020).

The mechanisms that underlie the link between offspring born to MO and HFDs being more prone to poor health outcomes are not yet fully elucidated. However, the obesity-induced suboptimal *in utero* environment lies at the root of the Developmental Origins of Adult Disease (DOHaD) hypothesis, which may provide a framework for inquiry. This hypothesis suggests that the environment to which one is exposed *in utero* contributes to the risk of non-communicable disease in later life (Barker, 2004; McMillen & Robinson, 2005).

In the case of MO and HFDs, there is an increased transfer of metabolic substrates to the fetus (Zhu et al., 2010). The fetal heart adapts to changes in available metabolic substrates to balance energy supply, expenditure, and substrate selection. A primary factor regulating this is circulating thyroid hormones (TH), namely triiodothyronine (T3) and thyroxine (T4), with the late gestation rise in fetal plasma T3 known to modulate cardiac metabolism through its regulation of oxidative phosphorylation and glucose metabolism (Chattergoon, 2019; Chattergoon et al., 2023; Nathanielsz & Fisher, 1979). Maternal HFDs can disrupt circulating TH concentration by impacting tissue-specific factors involved in T3 biosynthesis (Suter et al., 2012); however, whether a similar response to maternal HFD takes place within the fetal heart is not known.

In preclinical studies, there is evidence of altered insulin signalling in the hearts of fetal sheep (Wang et al., 2010) and reduced cardiac glucose uptake in rodent fetuses (Vaughan et al., 2022). There are reports of mitochondrial defects in rodent offspring exposed to maternal HFD (Mdaki et al., 2016; Turdi et al., 2013), which is a concern given that increased contractile demand after birth can only be met through mitochondrial oxidative phosphorylation (Dimasi et al., 2023b). Indeed, contractile dysfunction is evident in fetal sheep exposed to MO (Wang et al., 2010, 2019). There is evidence that this persists after birth in rodent offspring (Mdaki et al., 2016; Vaughan et al., 2022) and parallels pathological hypertrophy (Vaughan et al., 2022; Wang et al., 2010). Together, these effects have negative implications for cardiac health throughout the life course.

Whilst much knowledge has been gained through studies in sheep and rodents regarding the consequences of increased *in utero* substrate availability and offspring cardiac development, the non-human primate (NHP) is a valuable preclinical model for the study of MO and HFDs (Cox et al., 2013) due to the physiological and developmental similarities to humans (Huber et al.,

2020). In our baboon model of maternal HF-HED, we have previously shown altered fetal liver development and lipid accumulation in offspring (Puppala et al., 2018), disruption of the maternal and fetal methionine cycle (Nathanielsz et al., 2015), altered cardiac miRNA expression (Maloyan et al., 2013), and structural and functional changes to the placenta (Farley et al., 2009). In juvenile baboon offspring of maternal HF-HED, we have reported altered growth patterns (Li et al., 2019) and dysregulation of metabolic pathways in the liver, skeletal muscle, and plasma (Ampong et al., 2022). Herein, we aimed to investigate the impact of maternal high-fat–high-energy diet (HF-HED) exposure on TH concentrations and metabolic signalling pathways in the developing NHP fetal heart. We hypothesised that exposure to a maternal HF-HED *in utero* would alter the TH status and metabolic profile of the fetal heart.

Methods

Animal care and maintenance

All experimental protocols were approved by the Texas Biomedical Research Institute, University of Texas Health Science Centre at San Antonio Institutional Animal Care and Use Committee and conducted at the Southwest National Primate Research Centre (AAALAC International approved facility). All animal procedures abide by the United States Animal Welfare Act and were performed by fully certified MDs or DVMs. Protocols for the acquisition, analysis or interpretation of data within this paper were not pre-registered. The reporting of animal research in this paper adheres to the essential 10 ARRIVE guidelines (Kilkenny et al., 2010) and the principles of the 3Rs (Tannenbaum & Bennett, 2015). Baboons were sourced from a colony maintained by the Southwest National Primate Research Centre (SNPRC) at the Southwest Foundation for Biomedical Research (SFBR, San Antonio, TX, USA). Baboons were maintained in groups of up to 16 in custom-built outdoor facilities allowing full socialisation and free movement. Environmental enrichment, such as toys, perches and music, were regularly provided (Li et al., 2019).

Nutritional diet

Once stable groupings were confirmed, female baboons (*Papio hamadryas*) of similar age (∼11 years of age) and weight were randomly assigned to either a control diet ($n = 12$) or HF-HED ($n = 12$). One single fetus from each baboon pregnancy was considered an experimental unit. Diets started ∼9 months prior to mating and continued throughout pregnancy. Baboons had *ad libitum* access to water and the assigned diet. Both diets were made

available to the HF-HED group because baboons ate more HF-HED when it was provided together with the control diet as previously described (Li et al., 2019; Nathanielsz et al., 2015). The energy content of the control diet (Purina 5LEO; Purina LabDiets, St Louis, MO, USA) was derived from fat (14%), glucose (0.22%) and fructose (0.24%) and the metabolisable energy content (MEC) was 2.98 kcal/g. The energy content of the HF-HED (Purina 5045−6) was derived from fat (45%), glucose (4.6%) and fructose (5.6%) and the MEC was 4.03 kcal/g *ad libitum* with free access to a high fructose beverage.

Post-mortem and tissue collection

At 165 days' gestation (term ∼184 days), Caesarean sections were performed to deliver fetuses and collect cardiac samples. Caesarean sections were performed using a standard sterile surgical technique as previously described (Cox et al., 2006; Puppala et al., 2018). Briefly, baboons were pre-medicated with ketamine hydrochloride intramuscularly (Fort Dodge Animal Health, Fort Dodge, IA, USA; 10 mg/kg intramuscularly), intubated and maintained at a surgical plane of anaesthesia with isoflurane (2%) throughout the surgery. After the hysterectomy, the umbilical cord was identified and then used for fetal exsanguination under general anaesthesia as approved by the American Veterinary Medical Association Panel on Euthanasia (Puppala et al., 2018). Morphometrical measurements were collected, and tissue samples were obtained immediately after the placenta and fetus were removed from the uterus. Fetal body and heart weight measurements were recorded, left ventricle tissue was collected and snap-frozen in liquid nitrogen and stored at −80°C for molecular analysis. Buprenorphine hydrochloride (Hospira, Inc., Lake Forest, IL, USA; 0.2 mg/kg/day, 2 daily doses for 3 days) was administered for postoperative maternal analgesia. After recovery from anaesthesia, baboons were individually caged for the initial post-operative period and then group-housed for 90 days with a vasectomised male to prevent pregnancy before the surgical site was completely healed as previously described (Cox et al., 2006; Puppala et al., 2018; Schlabritz-Loutsevitch et al., 2004)

Quantification of gene expression in the left ventricle

Total RNA extraction. In a subset, RNA was extracted and purified from ∼50 to 100 mg of fetal heart tissue ($n = 3$ female (F), 6 male (M)) and HF-HED ($n = 6$ F, 6 M) using Qiagen QIAzol Lysis Reagent and the RNeasy Mini Kit (Qiagen Pty Ltd Australia, Doncaster, Australia) according to the manufacturer's protocol. The purity and concentration of RNA was measured at 260 and 280 nm using 2 μl of each sample on a spectrophotometer

and the integrity of the RNA was determined using agarose gel electrophoresis. The cDNA was synthesised using Superscript III (Thermo Fisher Scientific, Waltham, MA, USA) reverse transcription as previously described (Soo et al., 2012). To ensure RNA samples contained no double-stranded DNA, all samples were run on a no amplification control (NAC) plate.

Quantitative real-time PCR. All qRT-PCR procedures adhered to the MIQE guidelines (Bustin et al., 2009). The target genes were type 1 deiodinase iodothyronine (*DIO*)*1*, *DIO2* and *DIO3* and thyroid hormone receptors (TRs) TRα (*THRA*) and TRβ (*THRB*). The expression of target genes was normalised to three reference genes (listed in Table 1). Appropriate reference genes were determined by running samples on a plate that contained eight candidate reference genes and then selecting the three that were most stable across all samples using geNorm qbase software (Biogazelle, Belgium, Europe) (McGillick et al., 2013). Each sample was run in triplicate for each target and reference gene and the mRNA amplification for each sample was determined using Applied Biosystems Fast SYBR Green Master Mix (Thermo Fisher Scientific). Each well on the qRT-PCR plate contained 1 μl of cDNA, 3 μl Fast SYBR Green Master Mix (2×), and 2 μl of forward and reverse primer mixed with differing amounts of H_2O depending on the required final primer concentrations. No template controls (NTC) for each primer set were included on each plate to check for non-specific amplification. The threshold was set within the exponential growth phase of the amplification curve and the corresponding C_t values were obtained to quantify each reaction as previously described (McGillick et al., 2013; Soo et al., 2012).

Quantification of protein abundance in the fetal heart

Protein extraction. Protein was extracted from ∼100 mg of fetal heart tissue (control diet, $n = 6$ F, 6 M; HF-HED, $n = 6$ F, 6 M) using sonication (John Morris Scientific, Chatswood, NSW, Australia) in lysis buffer consisting of 1 ml/100 mg tissue of 1 mM Tris–HCl (pH 8, 5 M NaCl, 1% NP-40, 1 mM sodium orthovanadate, 30 mM NaF, 10 mM sodium tetrapyrophosphate, 10 mM EDTA) and a protease inhibitor tablet (complete Mini; Roche). Samples were then centrifuged at 14,300 *g* and 4°C for 14 min (Eppendorf Centrifuge 5415, Crown Scientific, Macquarie Park, NSW, Australia). A Pierce Micro BCA Protein Assay Kit (Thermo Fisher Scientific) was used to determine the protein content of each sample. Bovine serum albumin (BSA; 2 mg ml^{-1} stock solution) was used to make a standard curve. Samples were subsequently diluted to 5 mg/ml as previously described (Darby et al., 2018; Lie et al., 2014; Soo et al., 2012).

Table 1. Primer sequences used in quantitative real-time PCR to measure genes of interest

Gene	Forward	Reverse	Accession no.
Reference genes			
Hypoxanthine phosphoribosyl transferase (*HPRT*)	GTCCTATTGACATCGCCAGTAA	CCACCCAAAGGGAACTGATAG	XM_017954392.1
Beta-2-microglobulin (*B2M*)	AAGTGGGATCGAGACATGTAAG	CTGCCCAGATACCTCAAACA	NM_001173535.1
TATA box binding protein, transcript variant 1 (*TBP*)	GCTTCAGAGAGTTCTGGGATTG	GTGGTTCGTGGCTCTCTTATC	XM_009206461.4
Target genes			
Type 1 iodothyronine deiodinase (*DIO1*)	CAGGATCCTCTACAAGGGTAAATC	GGACACAGGTCAAAGGTAAGAG	XM.021941857.2
Type 2 iodothyronine deiodinase (*DIO2*)	CCATGTAGTGCTCTCAGTCTTC	TCCTCCCTAGCTTGTCAATTTC	XM.017961411.3
Type 3 iodothyronine deiodinase (*DIO3*)	CTACATCATCCCGCAGCAC	CGGCCACCTTGGTACATAATAG	XM.003919552.4
Thyroid hormone receptor alpha (*THRA*)	GCAAGTCACTCTCTGCCTTTA	GAAGTGCGGAATGTTGTGTTT	XM.009190540.4
Thyroid hormone receptor beta (*THRB*)	GGTCCTTGAAGAGAGCAAGAA	CTGTCATACTGTTGGGAGTCATAG	XM.017955953.3

Western blotting. Seventy-five micrograms of total protein from each sample was subjected to SDS-PAGE set at a constant 40 V. Proteins in each sample were then transferred at 800 mA constant onto a nitrocellulose membrane (Hybond ECL, GE Healthcare, Mascot, NSW, Australia). To assess the efficacy of the transfer and quantify the total protein on the membrane, membranes were subsequently stained with Ponceau S (0.5% Ponceau in 1% acetic acid) via agitation for 2 min followed by a brief wash with 7% acetic acid to distinguish total protein bands. Membranes were imaged using ImageQuant LAS 4000 (GE Healthcare Life Sciences) and total protein was quantified by densitometry using Image quant analysis software (GE Healthcare Life Sciences).

Membranes were then subjected to three 5-min washes in Tris-buffered saline (TBS) and then blocked in 5% BSA in TBS with 1% Tween (TBS-T) for 1 h at room temperature. The membranes then underwent three 5-min washes in TBS-T and were incubated with their respective primary antibody overnight at 4°C. The antibodies used were as follows: glucose transporter 4 (GLUT-4; 1:1000, ab33780, Abcam, Waltham, MA, USA; Wang et al., 2013), phosphorylated insulin receptor substrate 1 (pIRS1; 1:1000, cat. no. 2389, Cell Signaling Technology, Danvers, MA, USA; Darby et al., 2023), insulin receptor substrate 1 (IRS1; 1:1000, cat. no. 3194, Cell Signaling Technology; Lie et al., 2014), protein kinase B (Akt; 1:1000, cat. no. 9272, Cell Signaling Technology; Wang et al., 2013), phosphorylated protein kinase B (pAkt; T308; 1:1000, cat. no. 9275, Cell Signaling Technology), phosphorylated 160 kDa substrate of Akt (pAS160; 1:1000, cat. no. 4288S Cell Signaling Technology; Botting et al., 2018), 160 kDa substrate of Akt (AS160; 1:1000, cat. no. 2670, Cell Signaling Technology), Mitobiogenesis (1:250, ab123545, Abcam; Dimasi et al., 2023a), optic atrophy 1 (OPA1; 1:1000, cat. no. 80 471, Cell Signaling Technology), dynamin-related protein 1 (DRP1; 1:1000, cat. no. 8570, Cell Signaling Technology), Mitofusin-2 (1:1000, cat. no. 9482, Cell Signaling Technology), Total OXPHOS (1:1000, ab110413, Abcam; Darby et al., 2020), phosphorylated CaM-kinase II (pCAMKII, T286, 1:1000, ab171095, Abcam; Wang et al., 2013), CaM-kinase II (CAMKII; 1:1000, cat. no. 3362, Cell Signaling Technology; Wang et al., 2013), phospholamban (PLN; 1:1000, cat. no. 8495, Cell Signaling Technology; Darby et al., 2018), SERCA2 ATPase (SERCA; 1:1000, ab2861, Abcam; Wang et al., 2015), phosphorylated troponin I (pTroponin; Ser 23/24; 1:1000, cat. no. 4004S, Cell Signaling Technology; Darby et al., 2018), Troponin I (1:1000, ab19615, Abcam), peroxisome proliferator-activated receptor γ coactivator 1-α (PGC-1α; 1:1000, cat. no. 2178S, Cell Signaling Technology; Wang et al., 2013), carnitine palmitoyl transferase 1 (CPT1β; 1:200, sc-98 834, Santa Cruz Biotechnology, Dallas, TX, USA; Wang et al., 2013), fatty acid translocase cluster of differentiation 36 (CD36; 1:1000, ab133625, Abcam; Dimasi et al., 2023a), AMP-activate protein kinase (AMPK; 1:1000, cat. no. 2795, Cell Signaling Technology) and β-actin (ATCB, horseradish peroxidase (HRP) conjugate, Cell Signaling Technology). After incubation with the primary antibody, the membranes were subjected to three 5-min washes in TBS-T and incubated with the appropriate HRP-labelled secondary antibody specific to the species that the primary was raised in rabbit (1:2000, cat. no. 7074, Cell Signaling Technology) and mouse (1:2000,

cat. no. 7077, Cell Signaling Technology) antibody for 1 h at room temperature. Enhanced chemiluminescence using SuperSignal West Pico Chemiluminescent Substrate (Thermo Fisher Scientific) was used to detect the bands on the blots. The western blot was imaged using ImageQuant LAS 4000 (GE Healthcare Life sciences) and the protein abundance was quantified by densitometry using ImageQuant analysis software (GE Healthcare Life Sciences) and normalised to either β-actin or Ponceau S (total protein stain) as previously described (Darby et al., 2018; Lie et al., 2014; Soo et al., 2012).

Tissue hormone assay

Due to the amount of frozen tissue available, tissue hormone (cortisol, cortisone, 11-deoxycortisone, triiodothyronine (T3) and thyroxine (T4)) concentrations in a subset of animals (control diet, $n = 2$ F, 5 M; HF-HED, $n = 5$ F, 6 M) were determined by liquid chromatography (LC; Shimadzu Nexera XR, Shimadzu, Japan) coupled to a SCIEX 6500 Triple-Quad system (MS/MS; SCIEX, Framingham, MA, USA) using an adapted protocol (Dimasi et al., 2023b; Lock et al., 2023; McBride et al., 2020). Heart tissue was homogenised in 500 µl 0.9% NaCl at 50 hertz for 2 min and then centrifuged at 12,000 g for 10 min at 4°C. One hundred microlitres of supernatant was added to 300 µl acetonitrile containing 50 ng/ml internal standard (cortisol-9,11,12,12-d4; Toronto Research Chemicals, Toronto, Canada), vortexed for 1 min and then centrifuged at 12,000 g for 10 min. The supernatant was transferred to a fresh Eppendorf tube and the remaining pellet was resuspended in 300 µl ethyl acetate, vortexed for 1 min and then centrifuged at 12,000 g for 10 min. The supernatant was added to the acetonitrile, mixed by inversion, and then evaporated to dryness using the GeneVac EZ-2 Evaporating System (GeneVac, Ipswich, UK). Dried samples were reconstituted in 50% methanol and then injected into an ACQUITY UPLC BEH C18 Column 130 Å, 1.7 µm, 2.1 mm × 100 mm (Waters Corp, Milford, MA, USA). Mobile phases were 0.1% formic acid in water (A) and 0.1% formic acid in acetonitrile (B). The flow rate was 0.3 ml/min and mobile phase B was initially 10% and increased linearly to 90% over 10 min and then held at 90% for 2 min, after which it returned to 10% over 3 min before injection of the next sample. Hormone concentrations were calculated via integration with a standard curve that ranged from 0.05 to 100 ng/ml.

Statistical analysis

All statistical analyses were performed in GraphPad Prism version 8 (GraphPad Software, Inc., San Diego, CA, USA). Normality was assessed using a Shapiro–Wilk test where $P < 0.05$ indicated non-normality. Protein data were analysed using a two-way ANOVA (factors: diet and sex) with Bonferroni *post hoc* analysis. Due to limited tissue availability and thus unbalanced sex distribution between groups, no attempt was made to analyse tissue hormone concentrations and gene data via two-way ANOVA; instead, data were analysed using Student's unpaired *t*-test. Simple linear regressions were used to determine the relationship between hormone concentration and protein expression as well as maternal and fetal characteristics. Protein bands were excluded from analysis if pixels were highlighted in red, as this indicates that the signal intensity of the protein band exceeded the capacity of the imaging system, thereby preventing densitometry analysis. For tissue hormone analysis, the mean and SD of each sample triplicate were used to calculate the coefficient variation (CV) percentage of each sample, and those with a percentage error >15% were excluded. Outliers were identified using a 10% ROUT test and excluded (maximum one outlier per treatment group). Data are presented as means ± SD and a probability of ≤5% (i.e. $P \leq 0.05$) was considered significant for all analyses.

Results

Compared to controls, HF-HED mothers had higher body weight 30 days pre-conception ($P = 0.0026$; Fig. 1*A*) and on the day of post-mortem (PM; $P = 0.0029$; Fig. 1*B*). Maternal HF-HED had no impact on maternal weight gain during pregnancy ($P = 0.4493$; Fig. 1*C*). Maternal HF-HED had no impact on fetal weight; however, males were heavier than females irrespective of maternal diet ($P = 0.0492$; Fig. 1*D*). Maternal HF-HED had no impact on fetal heart weight ($P = 0.3669$; Fig. 1*E*). There were positive relationships between fetal weight and both maternal weight at PM ($P = 0.0039$, $R^2 = 0.5811$; Fig. 1*F*) and maternal weight gain ($P = 0.0046$, $R^2 = 0.6089$; Fig. 1*G*) in controls, but these associations were not apparent in the HF-HED group.

Maternal HF-HED impacted fetal cardiac concentration of thyroid hormone triiodothyronine (T3)

Maternal HF-HED reduced fetal cardiac concentrations of cortisone (Table 2; $P = 0.049$), but there was no impact on fetal cardiac concentrations of cortisol, 11-deoxycortisone, or the ratio of cortisol to cortisone (Table 2). Maternal HF-HED decreased fetal cardiac concentrations of T3 ($P = 0.0155$; Fig. 2*A*); but not T4 ($P = 0.0578$; Fig. 2*B*) or the ratio of T3:T4 ($P = 0.299$; Fig. 2*C*). Maternal HF-HED decreased the mRNA expression of *DIO1* ($P = 0.0251$; Fig. 2*D*), but not *DIO2* ($P = 0.585$; Fig. 2*E*), *DIO3* ($P = 0.206$; Fig. 2*F*), *THRA* ($P = 0.659$; Fig. 2*G*), or *THRB* ($P = 0.516$; Fig. 2*H*) in the fetal heart.

Maternal HF-HED decreased fetal cardiac insulin-mediated glucose signalling

Maternal HF-HED decreased pIRS1 relative to total IRS1 in the fetal heart in both sexes (pIRS1:IRS1; $P = 0.0128$; Fig. 3*A*). Maternal HF-HED did not change the abundance of pAkt relative to total Akt (pAkt:

Akt; $P = 0.0672$; Fig. 3*B*) or pAS160 relative to total AS160 (pAS160: AS160; $P = 0.1101$; Fig. 3*C*). However, HF-HED decreased the abundance of glucose transporter 4 (GLUT4) in the fetal heart in both sexes ($P = 0.0001$; Fig. 3*D*), although females had higher GLUT4 irrespective of diet ($P = 0.0256$; Fig. 3*D*). The concentration of cardiac T3 was positively correlated with the ratio of
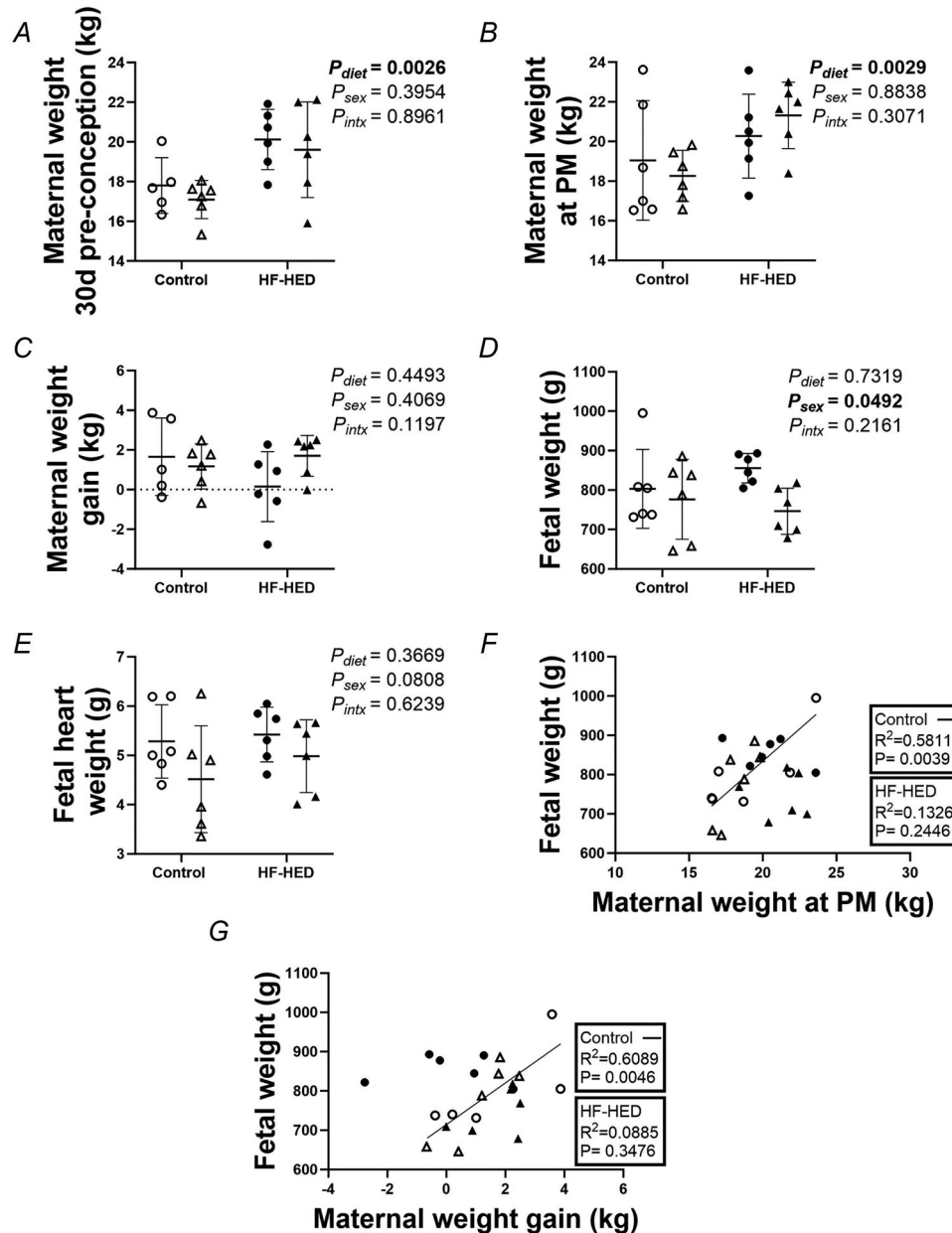

Figure 1. The impact of maternal HF-HED on maternal and fetal characteristics
A–E, the impact of maternal HF-HED on maternal weight for female and male fetuses 30 days pre-conception (*A*), maternal weight at post-mortem (*B*), maternal weight gain during pregnancy (*C*), fetal weight (*D*), and fetal heart weight (*E*). *F* and *G*, there was a relationship between fetal weight and both maternal weight at post-mortem and maternal weight gain in the control, but not HF-HED group. Each symbol represents an individual data point. Control, open symbols (*n* = 12); HF-HED, black symbols (*n* = 12). Circles, males; triangles, females. Data were analysed by a two-way ANOVA and linear regression. Data presented as means ± SD. *P* < 0.05 was considered statistically significant.

Table 2. The impact of Maternal HF-HED on fetal cardiac concentration of glucocorticoids

Fetal cardiac glucocorticoid concentrations	Control (n = 2 F, 5 M),	HF-HED (n = 5 F, 6 M)	P
Cortisol (ng/mg)	0.066 (0.060)	0.031 (0.009)	0.072
Cortisone (ng/mg)	0.281 (0.062)	0.226 ± 0.066	**0.049**
Cortisol: cortisone	0.220 (0.176)	0.152 (0.045)	0.2328
11-Deoxycortisone (ng/mg)	0.062 (0.042)	0.0037 (0.001)	0.0828

Data expressed as means ± SD. Data were analysed by unpaired t test. $P < 0.05$ was considered significant (shown in bold).

pIRS1:IRS1 ($P = 0.0437$, $R^2 = 0.7902$; Fig. 3E) and GLUT4 ($P = 0.0416$, $R^2 = 0.6864$; Fig. 3F) in control fetuses, but not those from the HF-HED group.

Maternal HF-HED increased fetal cardiac mitochondrial electron transport chain complexes

Maternal HF-HED increased abundance of oxidative phosphorylation (OXPHOS) complex I (COXI; $P = 0.0045$; Fig. 4A), III (COXIII; $P = 0.0071$; Fig. 4C) and IV (COXIV; $P = 0.0074$; Fig. 4D) in the fetal heart in both sexes. Maternal HF-HED did not change the abundance of COXII ($P = 0.5152$; Fig. 4B) or COXV ($P = 0.3356$; Fig. 4E). The concentration of cardiac T3 was negatively correlated with COXI ($P = 0.0320$, $R^2 = 0.7226$; Fig. 4F), but only in the heart of control fetuses.

Maternal HF-HED increased fetal cardiac mitochondrial abundance and mitochondrial fission marker

Maternal HF-HED increased mitochondrial abundance, determined by a ratio of mitochondria DNA-encoded COX-I to nuclear DNA-encoded COXII as previously described (Dimasi et al., 2023a; $P = 0.0004$; Fig. 5A) in the fetal heart of both sexes. Mitochondrial fission marker DRP1 was increased in HF-HED males only ($P = 0.0178$; Fig. 5B). Maternal HF-HED had no impact on inner membrane mitochondrial fusion marker OPA1 ($P = 0.1738$; Fig. 5C) or outer membrane fusion marker Mitofusin-2 ($P = 0.4456$; Fig. 5D) in the fetal heart.

Sex-specific differences in fetal cardiac fatty acid transporter CD36 abundance

Maternal HF-HED did not change the abundance of mitochondrial biogenesis regulator PGC1α ($P = 0.3197$; Fig. 6A) or mitochondrial fatty acid transporter CPTI ($P = 0.1384$; Fig. 6B) in the fetal heart. CD36 protein abundance was higher in females compared with males independent of maternal diet ($P = 0.0404$; Fig. 6C), but there was no effect of maternal HF-HED. Maternal HF-HED had no impact on the abundance of AMPKα ($P = 0.6328$; Fig. 6D) in the fetal heart.

Maternal HF-HED impacted the abundance of molecules involved in fetal cardiac calcium handling in a sex-specific manner

Maternal HF-HED had no impact on the abundance of pTroponin I relative to total Troponin I ($P = 0.9806$; Fig. 7A), pCAMKIII relative to total CAMKII ($P = 0.4768$; Fig. 7B) and SERCA ($P = 0.5008$; Fig. 7C) in the fetal heart. The abundance of PLN was decreased in the fetal heart of HF-HED compared to control, but only in females ($P = 0.0171$; Fig. 6D).

Discussion

In this study, we investigated the impact of a maternal HF-HED, beginning before and continuing throughout pregnancy, on the TH status and cardiometabolic profile of the fetal heart. Whilst mothers consuming HF-HED did not gain weight during pregnancy on average (Meakin et al., 2024), they had an obesogenic phenotype in the pre-pregnancy period characterised by higher body weight, body fat percentage, waist-hip circumference, LDL-cholesterol, and triglycerides compared to controls (Nathanielsz et al., 2015). Despite no changes in maternal weight gain during pregnancy, we show that the relationship between maternal weight gain and fetal weight is dysregulated in HF-HED fetuses compared to controls. The data herein identified that the TH status of the fetal heart is sensitive to changes in substrate availability and likely contributes to the emergence of a cardiac insulin-resistant phenotype. Despite the HF-HED, fetal body weight was unchanged, suggesting that neonates with poor cardiometabolic profiles may go undetected in the clinical setting. It may also suggest that cardiometabolic phenotypes are more severe in neonates born with higher birth weights in response to MO.

Development of the fetal thyroid gland by mid-gestation is essential to produce TH with the late gestational rise in fetal plasma T3 (Nathanielsz &

Fisher, 1979) that promotes the maturation of cardiac growth and metabolic profiles (Chattergoon, 2019; Chattergoon et al., 2023). However, circulating fetal TH, the thyrotropin-releasing hormone in the hypothalamus, and genes necessary for TH production in the thyroid gland are reduced by maternal HF-HED diet in NHPs (Suter et al., 2012). In the present study, we showed that maternal HF-HED had no impact on fetal cardiac
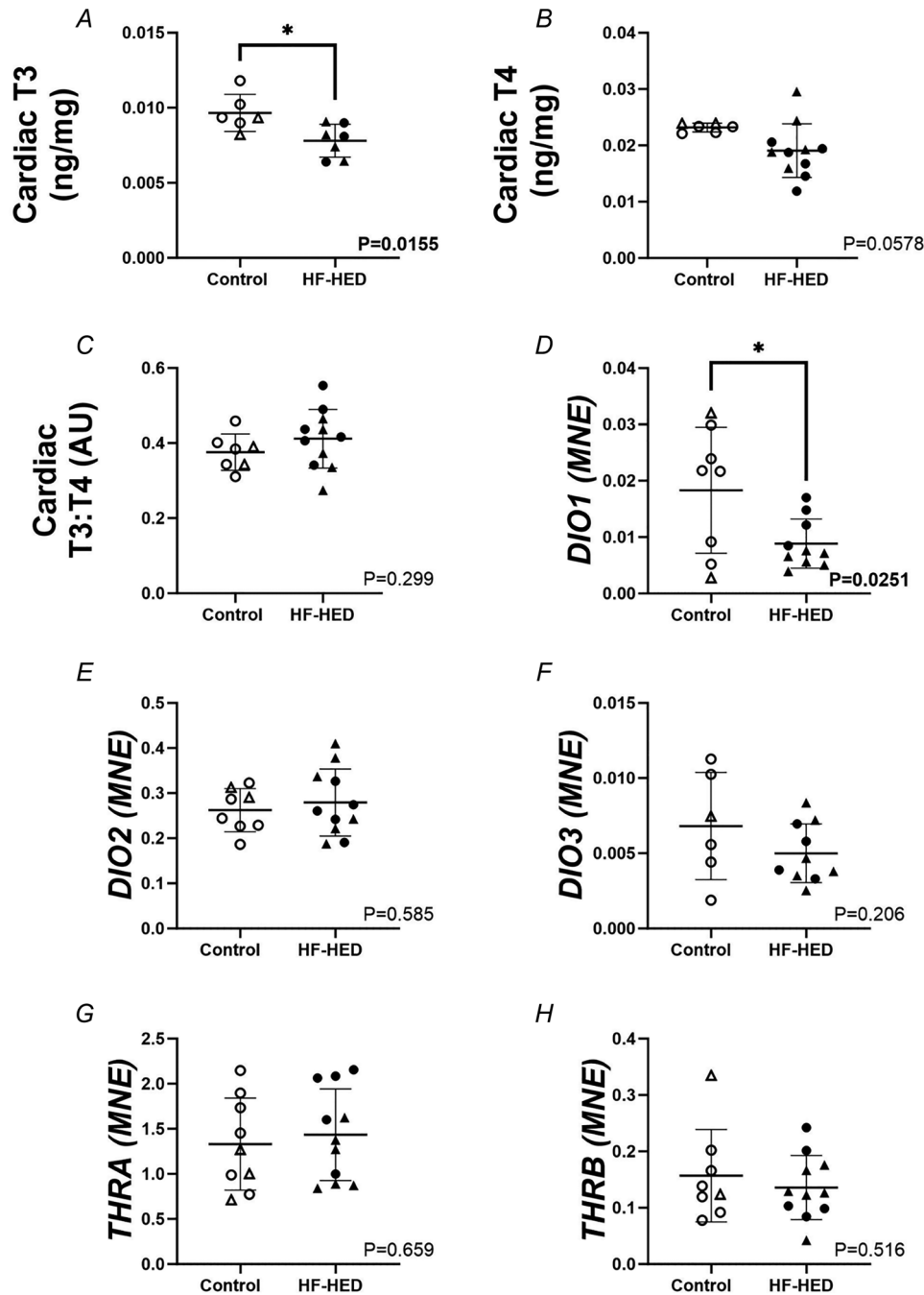

Figure 2. The impact of maternal HF-HED on fetal cardiac TH concentrations and genes regulating TH metabolism
A–C, the impact of maternal HF-HED on fetal cardiac T3 (*A*) and T4 concentration (*B*), and the ratio of cardiac T3:T4 (*C*). *D–H*, the impact of maternal HF-HED on mRNA expression of *DIO1* (*D*), *DIO2* (*E*), *DIO3* (*F*), *THRA* (*G*), and *THRB* (*H*). Each symbol represents an individual data point. Control, open symbols (hormones, *n* = 7; gene, *n* = 9); HF-HED, filled symbols (hormones, *n* = 11; gene, *n* = 12). Circles, males; triangles, females. Data were analysed by a *t* test. Data presented as means ± SD. *P* < 0.05 was considered statistically significant.
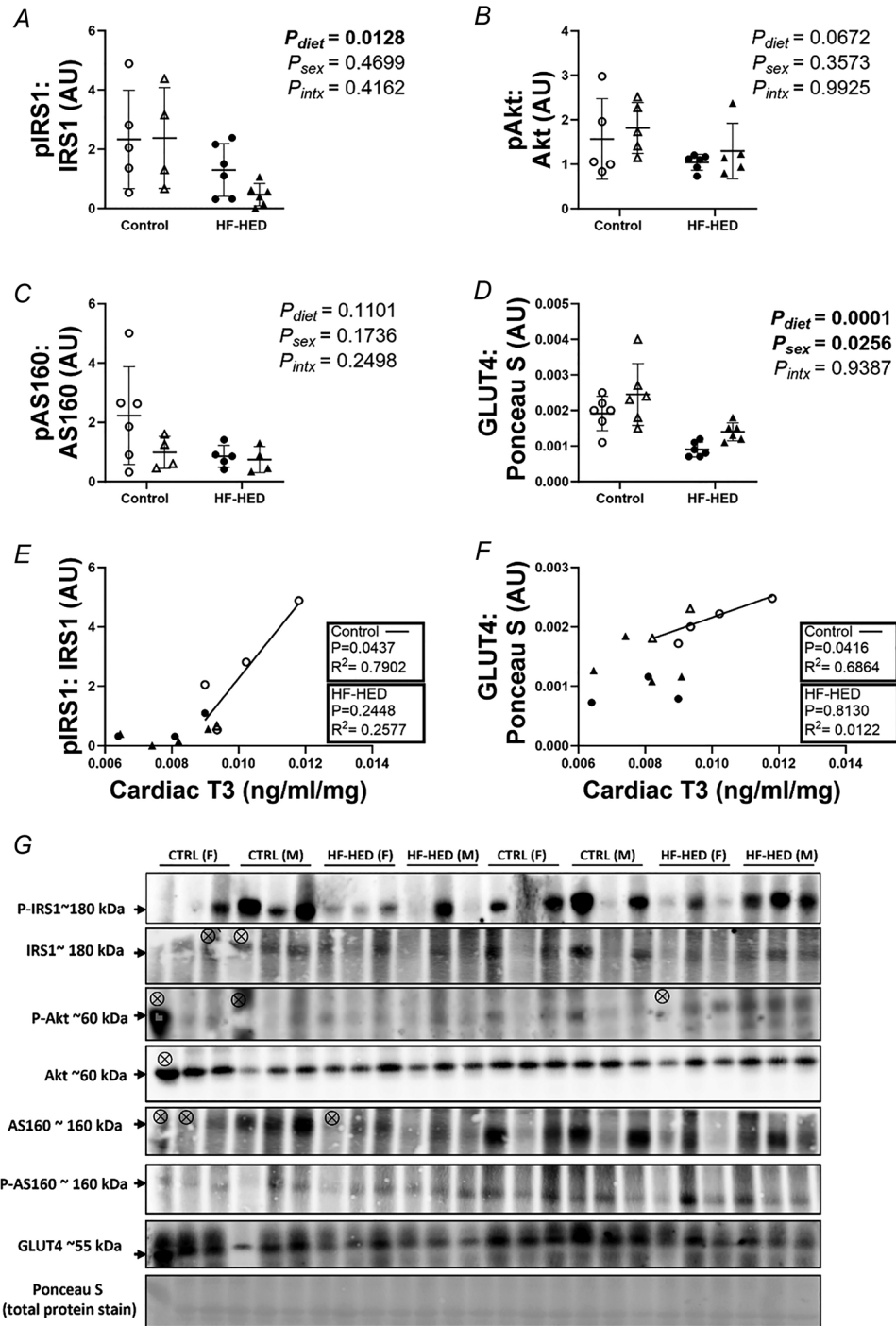
Figure 3. The impact of maternal HF-HED on markers of fetal cardiac insulin-mediated glucose signalling
A–D, the effect of maternal HF-HED on protein abundance of phosphorylated IRS1 relative to total IRS1 (*A*), phosphorylated Akt relative to total Akt (*B*), phosphorylated AS160 relative to total AS160 (*C*), and GLUT4 (*D*) in the fetal heart. *E* and *F*, there was a relationship between cardiac T3 and both pIRS1:IRS1 (*E*) and GLUT4 (*F*), but only in control fetuses. Each symbol represents an individual data point. Control, open symbols (*n* = 12); HF-HED, filled symbols (*n* = 12). Circles, males; triangles, females. Data presented as normalised protein expression in arbitrary units (AU). *G*, western blot images represent the target protein and reference protein for controls (CTRL) and HF-HED. ⊗: outlier excluded from the blot (red pixels indicate signal saturation) and not included in analysis for this study. Ponceau S (total protein stain) is a representative image of stains performed on each gel for protein normalisation. Data analysed by a two-way ANOVA and linear regression. Data presented as means ± SD. *P* < 0.05 considered statistically significant.
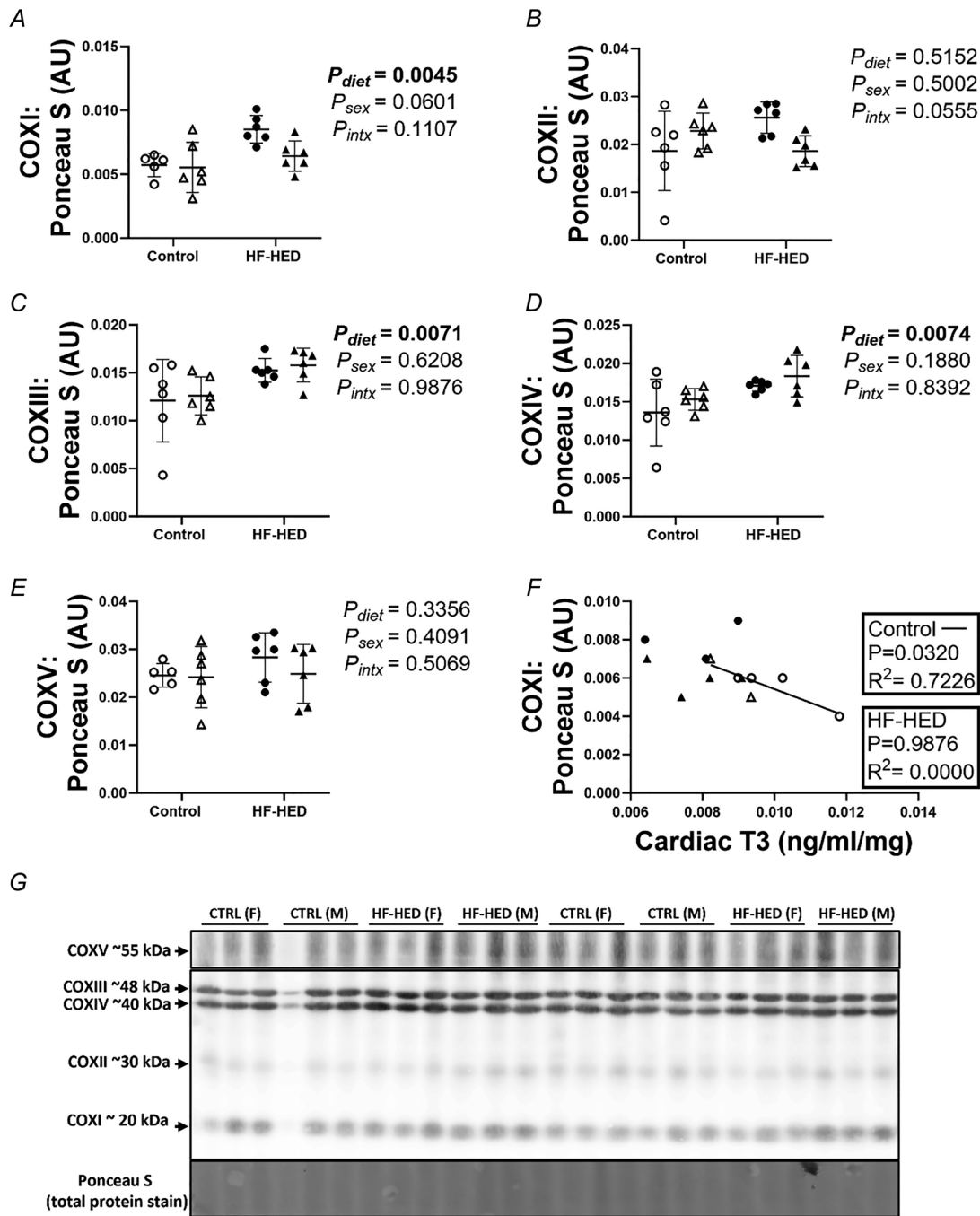
Figure 4. The impact of maternal HF-HED on markers of fetal cardiac mitochondrial electron transport chain complexes

A–F, the effect of maternal HF-HED on oxidative phosphorylation complexes COXI (*A*), COXII (*B*), COXIII (*C*), COXIV (*D*), and COXV (*E*) and the relationship between cardiac T3 and COXI present in controls only (*F*). Each symbol represents an individual data point. Control, open symbols (*n* = 12); HF-HED, filled symbols (*n* = 12). Circles, males; triangles, females. Data presented as normalised protein expression in arbitrary units (AU). *G*, western blot images represent the target protein and reference protein for controls (CTRL) and HF-HED. Ponceau S (total protein stain) is a representative image of stains performed on each gel for protein normalisation. Data were analysed by a two-way ANOVA and linear regression. Data presented as mean ± SD. *P* < 0.05 considered statistically significant.

concentrations of T4; however, the biologically active TH, T3, was reduced. Given that genes necessary for T3 and T4 production are decreased in the hypothalamus and thyroid gland by HF-HED (Suter et al., 2012), our cardiac findings may be indicative of reduced entry of plasma-derived T3 into the fetal heart. Alternatively, reduced T3 concentrations within the heart may be a result of maternal HF-HED-induced reduction in the activity of deiodinase (DIO) enzymes DIO1, DIO2, and DIO3 in the heart (Janssen et al., 2017). Specifically, DIO1/DIO2 are responsible for the conversion of T4 to T3, and thus, their activity contributes to cellular T3 concentrations (Janssen et al., 2017). The work of Suter et al. (2012) suggests that the hypothalamic–pituitary–thyroid axis is disrupted in response to maternal HFD, with DIO2 and DIO3 increased in the thyroid gland and DIO3
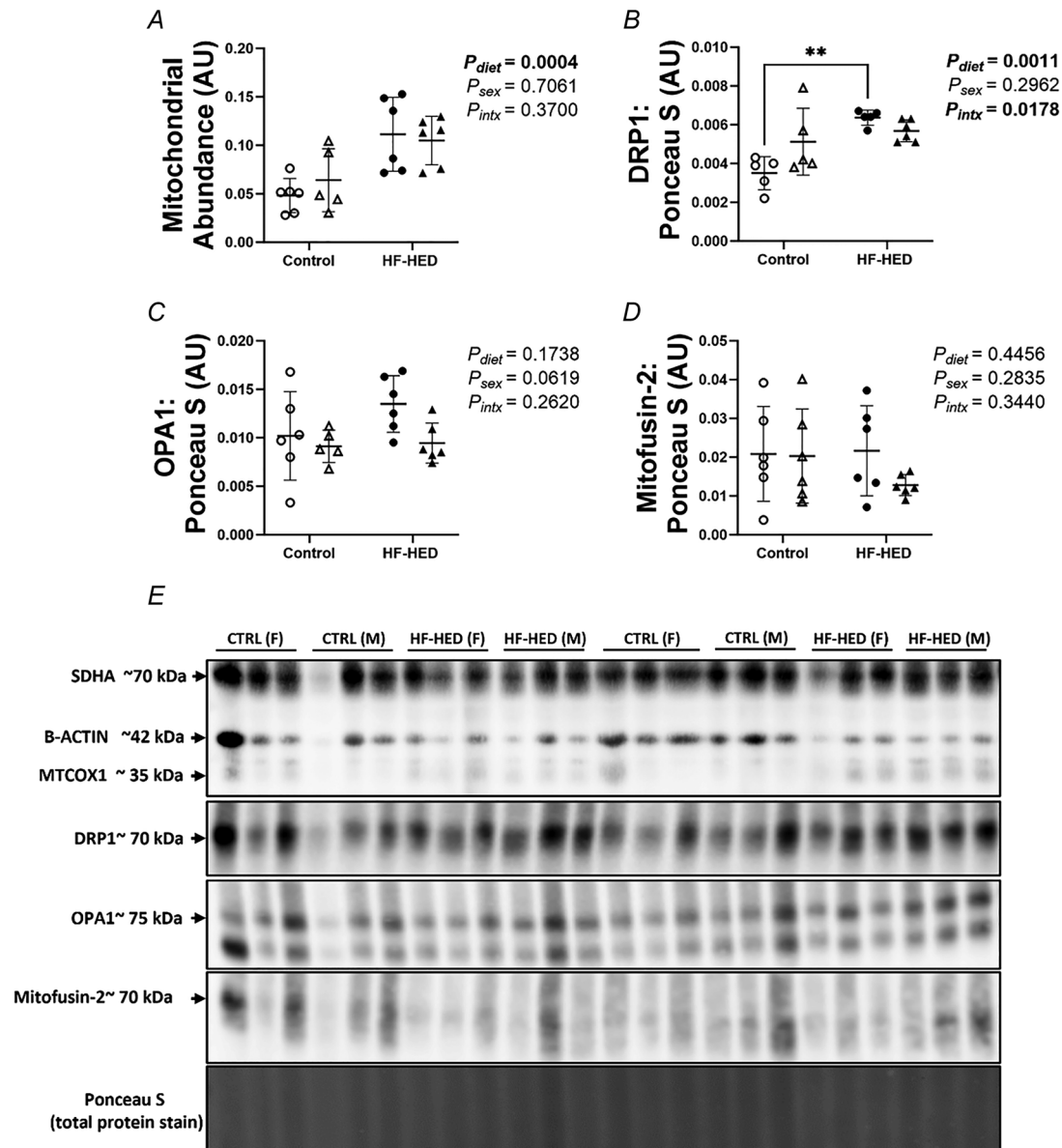

Figure 5. The impact of maternal HF-HED on markers of fetal cardiac mitochondrial abundance and markers of mitochondrial dynamics
A–D, the effect of maternal HF-HED on mitochondrial abundance (MTCOXI:SDHA; *A*), DRP1 (*B*), OPA1 (*C*), and Mitofusin-2 (*D*) in the fetal heart. Each symbol represents an individual data point. Control, open symbols ($n = 12$); HF-HED, filled symbols ($n = 12$). Circles, males; triangles, females. Data presented as normalised protein expression in arbitrary units (AU). *E*, western blot images represent the target protein and reference protein for controls (CTRL) and HF-HED. Ponceau S (total protein stain) is a representative image of stains performed on each gel for protein normalisation. Data were analysed by a two-way ANOVA. Data presented as means ± SD. $P < 0.05$ considered statistically significant.

decreased in the hypothalamus. Our data support these previous findings; specifically, we showed that fetal cardiac DIO1 expression was reduced in response to maternal HF-HED. A decrease in DIO1 may indicate less T3 derived from DIO1 deiodination, thereby contributing to reduced T3 concentrations within the heart of HF-HED fetuses. Whilst we report no changes in DIO2, the underlying distinction between DIO1-generated T3 and DIO2-generated T3 among different tissue types is not fully elucidated; however, there are reports that cardiac DIO2 contributes little to cardiac T3 concentrations (Pachucki et al., 2001).

Importantly, T3 impacts insulin-sensitive pathways by contributing to IRS1 phosphorylation (Lin & Sun, 2011) and cardiac regulation of GLUT4 expression (Castelló

et al., 1994). Any changes to insulin-mediated glucose uptake via reduced cardiac T3 impact the fetal heart, which under normal *in utero* conditions, utilises glucose as the primary metabolic substrate for ATP production (Pascual & Coleman, 2016). Indeed, our data suggest that a maternal HF-HED disrupts insulin-mediated glucose uptake in fetal hearts with decreased protein abundance of pIRS1 at ser789 and GLUT4. Consistent with the role of T3 in regulating metabolism, we show that the physiological relationship between cardiac T3 and pIRS1 and GLUT4 is dysregulated in HF-HED fetuses compared to controls, such that reduced cardiac T3 concentrations in response to HF-HED may impair these signalling pathways. Given that pIRS1 and GLUT4 are involved in the initial steps of insulin-mediated glucose transport
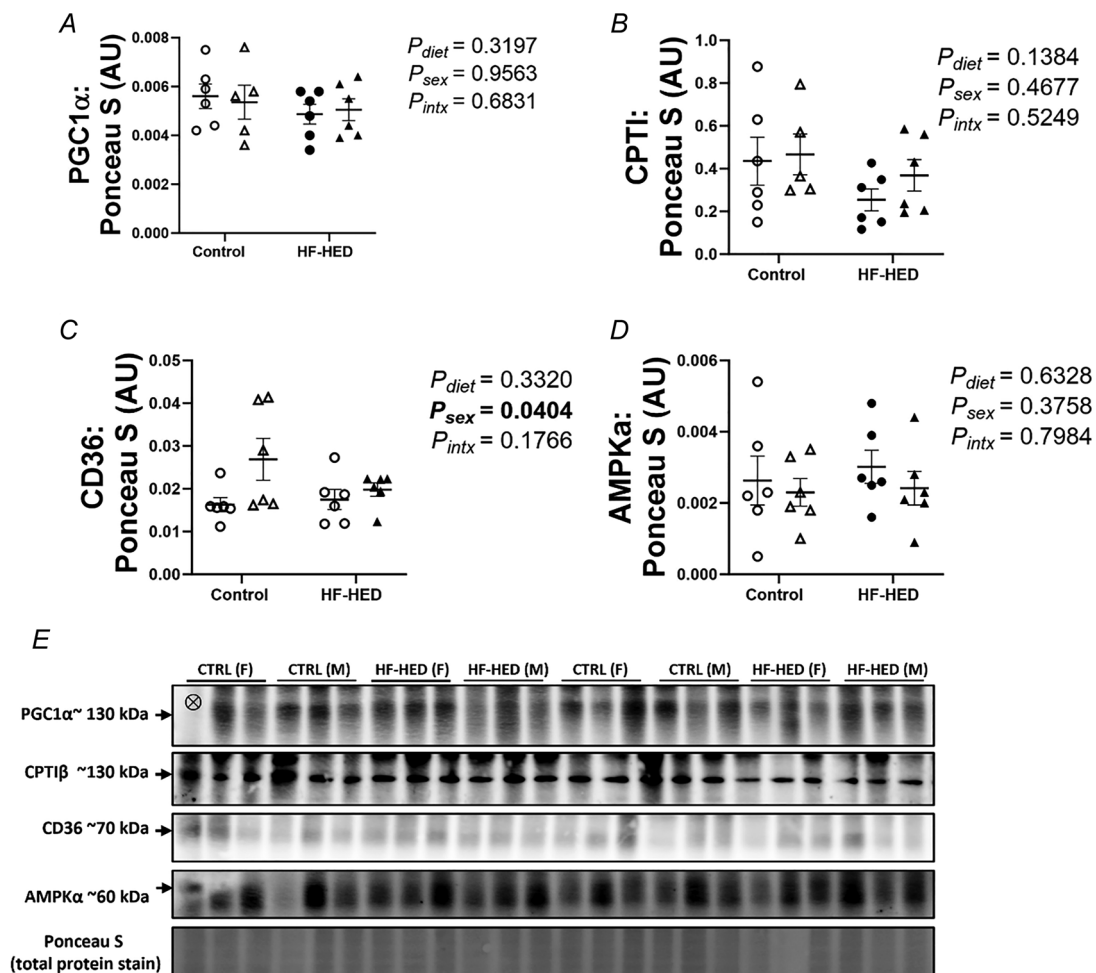

Figure 6. The impact of maternal HF-HED on markers of fetal mitochondrial biogenesis, fatty acid transport and energy sensing
A–D, the effect of maternal HF-HED on the protein abundance of PGC1α (*A*), CPTI (*B*), CD36 (*C*), and AMPKα (*D*) in the fetal heart. Each symbol represents an individual data point. Control, open symbols (*n* = 12); HF-HED, filled symbols (*n* = 12). Circles, males; triangles, females. Data presented as normalised protein expression in arbitrary units (AU). *E*, western blot images represent the target protein and reference protein for controls (CTRL) and HF-HED. ⊗: outlier excluded from the blot and not included in analysis for this study. Ponceau S (total protein) stains were performed on each membrane for protein normalisation. Data were analysed by a two-way ANOVA. Data presented as means ± SD. *P* < 0.05 was considered significant.

(Pascual & Coleman, 2016), the HF-HED-induced suppression of IRS1 activation and GLUT4 abundance in fetal hearts may be the early emergence of cardiac insulin resistance as reported in the heart of sheep fetuses exposed to MO (Wang et al., 2010). This aligns with rodent models where MO reduces cardiac glucose uptake *in utero* (Vaughan et al., 2022) and programs cardiac insulin resistance in both rodent offspring (Mdaki et al., 2016; Turdi et al., 2013) and early adulthood piglets (Guzzardi et al., 2018). Increased blood insulin concentrations in these HF-HED fetuses (Puppala et al., 2018) may be mediating this dysregulation of insulin-mediated glucose uptake within the heart. Importantly, cardiac insulin resistance often precedes whole-body insulin resistance,
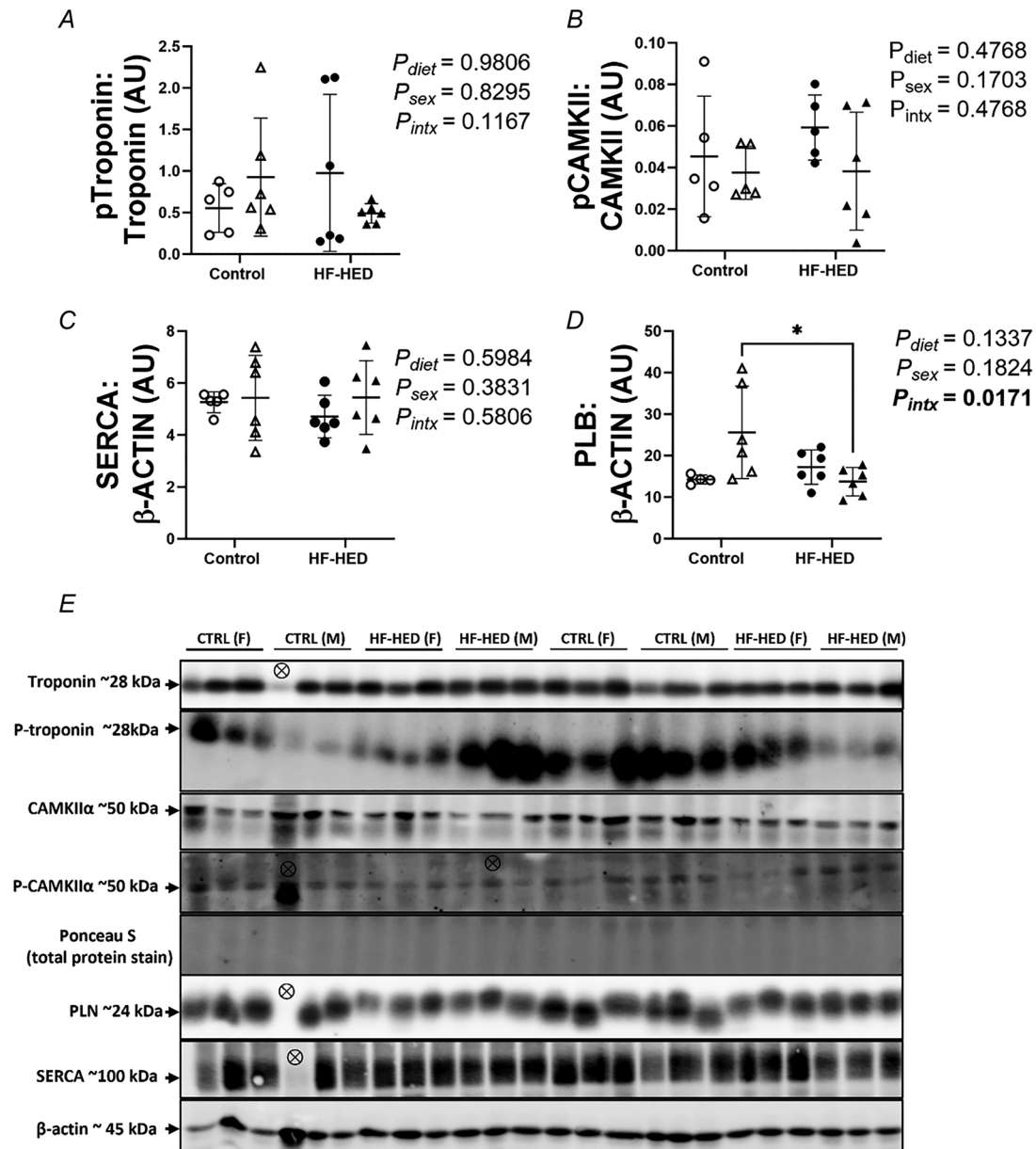

Figure 7. The impact of maternal HF-HED on markers of fetal cardiac contractility
A–D, the effect of maternal HF-HED on the ratio of phospho-Troponin I:total Troponin I (*A*), the ratio of phosphorylated CAMKII:total CAMKII (*B*), SERCA (*C*), and phospholamban (*D*) in the fetal heart. Each symbol represents an individual data point. Control, open symbols ($n = 12$); HF-HED, black symbols ($n = 12$). Circles, males; triangles, females. Data presented as normalised protein expression in arbitrary units (AU). *E*, western blot images represent the target protein and reference protein for controls (CTRL) and HF-HED. ⊗: outlier excluded from the blot and not included in analysis for this study. β-Actin or Ponceau S (total protein stain) was used for protein normalisation. Data were analysed by a two-way ANOVA. Data presented as means ± SD. $P < 0.05$ considered statistically significant.

and when clustered with conditions such as hypertension, diabetes, and obesity, there is a higher risk of heart failure in later life (Aroor et al., 2012). Moreover, fetal exposure to HFD and MO is associated with an increased risk of CVD in adulthood, which may have its origins in the development of subclinical insulin resistance *in utero* (Lee et al., 2015; Zambrano & Nathanielsz, 2013).

Whilst reduced T3 concentrations may have directly reduced markers of glucose utilisation, this suppression may also be a result of an increased abundance of an alternative substrate. Indeed, Randle and colleagues described the dynamic interaction between glucose and fatty acids (FAs) as competing substrates for fuel selection by mammalian organs, particularly the heart (Randle, 1998). This hypothesis states that insulin-mediated glucose signalling and translocation of GLUT4 is inhibited when there is increased oxidation of free FAs via OXPHOS. Moreover, underlying the reduced T3 concentrations in these HF-HED fetal hearts may be increased mitochondrial OXPHOS activity inducing a suppression in the conversion of T4 to T3 (Forhead & Fowden, 2014). Indeed, we show that mitochondrial OXPHOS complexes I, III, and IV, the site of FA oxidation, are upregulated in fetal hearts from HF-HED pregnancies, suggesting an increased reliance on oxidative metabolism. Like the reduced GLUT4 abundance, changes in OXPHOS complexes may be associated with reduced T3 concentrations acting on the expression of mitochondrial OXPHOS (Forhead & Fowden, 2014). This is supported by the normal relationship between cardiac T3 and COXI being dysregulated in HF-HED fetuses compared to controls (Fig. 4*F*).

Impairments to mitochondrial biogenesis play a role in the pathophysiology of mitochondrial dysfunction and cardiometabolic syndrome (Nisoli et al., 2007). We show here that mitochondrial abundance is increased in HF-HED fetal hearts. This aligns with increased mitochondrial copy numbers in the hearts of rodent offspring exposed to MO (Mdaki et al., 2016). Signs of mitochondrial dysfunction have been reported in rodent offspring exposed to MO (Turdi et al., 2013). Therefore our data may suggest the early developmental signs of mitochondrial dysfunction in fetal life. Consistent with the notion that fetal hearts from HF-HED pregnancies may be at risk for the development of cardiac insulin resistance, mitochondrial dysfunction is well known to contribute to the pathophysiology of insulin resistance and heart failure (Aroor et al., 2012).

Taken together, the decrease in glucose uptake may have induced a compensatory mechanism acting to increase FA oxidation (Randle, 1998). Whilst this premature transition to OXPHOS *in utero* may seem beneficial for the adult heart that primarily utilises OXPHOS for energy production, there are circumstances during stress such as ischaemia, increased workload, and pressure overload-induced hypertrophy where a switch to glucose oxidation is necessary (Pascual & Coleman, 2016). Although beyond the scope of the present study, the downregulation of insulin-mediated glucose uptake *in utero*, if programmed to continue after birth, may reduce the metabolic flexibility of the adult heart and contribute to the development of cardiometabolic disorders (Smith et al., 2018). Indeed, the metabolic perturbations in the liver and skeletal muscle of these juvenile HF-HED offspring (Ampong et al., 2022) suggest that our findings of dysregulated metabolic factors in the present study are likely programmed to persist in the HF-HED offspring heart.

Importantly, there are sex differences in developmental programming in response to MO and HFDs (Meakin et al., 2024; Zambrano & Nathanielsz, 2013), a contributing factor to sex differences in cardiac dysfunction in later life (Maas & Appelman, 2010). Underlying this may be sex differences in the programming of mitochondrial dynamics in response to HF-HED. We report an increase in the mitochondrial fission marker DRP1 in male but not female fetuses exposed to HF-HED, indicating excessive mitochondrial fission and mitochondrial dysfunction (Serasinghe & Chipuk, 2017). This, in part, explains the increased mitochondrial abundance in HF-HED males; however, the mechanism underlying this change in the hearts of females exposed to HF-HED remains unclear as we report no differences in mitochondrial biogenesis regulator PGC1α (Serasinghe & Chipuk, 2017). One mechanism may be sex differences in cardiac T3 that also regulate mitochondrial biogenesis (Weitzel et al., 2003); however, we were unable to assess the effect of sex on cardiac T3 concentrations due to limited biospecimen sample availability. Indeed, future studies would benefit from examining the impact of maternal HF-HED and fetal sex on cardiac-specific TH signalling pathways.

Our finding that the protein abundance of fatty acid transporter CD36 is higher in females compared to males, independent of diet, suggests lipid handling processes and coordination of fat utilisation occur in a sex-dependent manner. We also report a sex-specific response to maternal HF-HED with females having reduced protein abundance of contractility marker PLN. The decrease in PLN in females may suggest calcium handling alterations and excitation–contraction coupling in response to HF-HED. These findings contrast with those in sheep models of MO that reported PLN increased in the fetal heart (Wang et al., 2019); however, the impact of sex was not assessed. In rodent models of MO, reduced PLN is associated with diastolic dysfunction, but only in male offspring (do Carmo et al., 2021). Collectively, our data suggest there are sex differences in the developmental programming of PLN in response to MO that may have functional consequences for the offspring's heart. Specifically, the decrease in PLN

in HF-HED female fetuses in the present study may serve protectively in maintaining diastolic function after birth.

This study is not without limitations. There is no fetal cardiac function data; however, obtaining these measures from magnetic resonance imaging (MRI) for NHP fetuses was not feasible as the fetal heart rate could not be used to trigger the MRI (Duan et al., 2019). Therefore, molecular findings could not be correlated with functional changes in the fetal heart. We were not able to assess sex effects in gene and hormone measures. Furthermore, it remains unclear if the altered cardiometabolic profile induced by maternal HF-HED results in the early emergence of cardiac dysfunction in fetal life and whether this later manifests in the offspring. Longitudinal follow-up studies to assess offspring outcomes during postnatal development and ageing are ongoing.

Conclusion

Maternal HF-HED prior to and throughout pregnancy induces a premature switch in fetal metabolic substrate preference from glucose to fatty acids. This altered cardiometabolic profile may be modulated by fetal TH status and predisposes the adult heart to reduced metabolic flexibility and cardiac insulin resistance that will exacerbate the risk of cardiometabolic disorders. Concerningly, these molecular markers of poor cardiac outcomes occur despite a normal fetal body weight. This raises concern for babies born from pregnancies complicated by MO with normal birth weights not being identified as having a future risk of poor cardiovascular health across the life course. Collectively, our data supports a growing dialogue around improved nutritional status prior to and throughout pregnancy and promotes the need for dietary interventions that will prevent adverse fetal metabolic programming and minimize the transgenerational impacts of insulin resistance and cardiometabolic disorders.

References

Ampong, I., Zimmerman, K. D., Perumalla, D. S., Wallis, K. E., Li, G., Huber, H. F., Li, C., Nathanielsz, P. W., Cox, L. A., & Olivier, M. (2022). Maternal obesity alters offspring liver and skeletal muscle metabolism in early post-puberty despite maintaining a normal post-weaning dietary lifestyle. *Federation of American Societies for Experimental Biology Journal*, **36**(12), e22644.

Aroor, A. R., Mandavia, C. H., & Sowers, J. R. (2012). Insulin resistance and heart failure: Molecular mechanisms. *Heart Failure Clinic*, **8**(4), 609–617.

Barker, D. J. (2004). The developmental origins of adult disease. *Journal of the American College of Nutrition*, **23**, (6 Suppl), 588S–595S.

Botting, K. J., Loke, X. Y., Zhang, S., Andersen, J. B., Nyengaard, J. R., & Morrison, J. L. (2018). IUGR decreases cardiomyocyte endowment and alters cardiac metabolism in a sex- and cause-of-IUGR-specific manner. *American Journal of Physiology- Regulatory, Integrative and Comparative Physiology*, **315**(1), R48–R67.

Bustin, S. A., Benes, V., Garson, J. A., Hellemans, J., Huggett, J., Kubista, M., Mueller, R., Nolan, T., Pfaffl, M. W., Shipley, G. L., Vandesompele, J., & Wittwer, C. T. (2009). The MIQE guidelines: Minimum information for publication of quantitative real-time PCR experiments. *Clinical Chemistry*, **55**(4), 611–622.

Castelló, A., Rodríguez-Manzaneque, J. C., Camps, M., Pérez-Castillo, A., Testar, X., Palacín, M., Santos, A., & Zorzano, A. (1994). Perinatal hypothyroidism impairs the normal transition of GLUT4 and GLUT1 glucose transporters from fetal to neonatal levels in heart and brown adipose tissue. Evidence for tissue-specific regulation of GLUT4 expression by thyroid hormone. *Journal of Biological Chemistry*, **269**(8), 5905–5912.

Chattergoon, N., Louey, S., Jonker, S. S., & Thornburg, K. L. (2023). Thyroid hormone increases fatty acid use in fetal ovine cardiac myocytes. *Physiological Reports*, **11**(22), e15865.

Chattergoon, N. N. (2019). Thyroid hormone signaling and consequences for cardiac development. *Journal of Endocrinology*, **242**(1), T145–T160.

Cox, L. A., Comuzzie, A. G., Havill, L. M., Karere, G. M., Spradling, K. D., Mahaney, M. C., Nathanielsz, P. W., Nicolella, D. P., Shade, R. E., Voruganti, S., & VandeBerg, J. L. (2013). Baboons as a model to study genetics and epigenetics of human disease. *Institute for Laboratory Animal Research Journal*, **54**(2), 106–121.

Cox, L. A., Schlabritz-Loutsevitch, N., Hubbard, G. B., Nijland, M. J., McDonald, T. J., & Nathanielsz, P. W. (2006). Gene expression profile differences in left and right liver lobes from mid-gestation fetal baboons: A cautionary tale. *The Journal of Physiology*, **572**(Pt 1), 59–66.

Darby, J. R. T., McMillen, I. C., & Morrison, J. L. (2018). Maternal undernutrition in late gestation increases IGF2 signalling molecules and collagen deposition in the right ventricle of the fetal sheep heart. *The Journal of Physiology*, **596**(12), 2345–2358.

Darby, J. R. T., Sorvina, A., Bader, C. A., Lock, M. C., Soo, J. Y., Holman, S. L., Seed, M., Kuchel, T., Brooks, D. A., Plush, S. E., & Morrison, J. L. (2020). Detecting metabolic differences in fetal and adult sheep adipose and skeletal muscle tissues. *Journal of Biophotonics*, **13**(3), e201960085.

Darby, J. R. T., Zhang, S., Holman, S. L., Muhlhausler, B. S., McMillen, I. C., & Morrison, J. L. (2023). Cardiac growth and metabolism of the fetal sheep are not vulnerable to a 10 day increase in fetal glucose and insulin concentrations during late gestation. *Heliyon*, **9**(7), e18292.

Dimasi, C. G., Darby, J. R. T., Cho, S. K. S., Saini, B. S., Holman, S. L., Meakin, A. S., Wiese, M. D., Macgowan, C. K., Seed, M., & Morrison, J. L. (2023a). Reduced in utero substrate supply decreases mitochondrial abundance and alters the expression of metabolic signalling molecules in the fetal sheep heart. *The Journal of Physiology*. Advance online publication. https://doi.org/10.1113/JP285572

Dimasi, C. G., Darby, J. R. T., & Morrison, J. L. (2023b). A change of heart: Understanding the mechanisms regulating cardiac proliferation and metabolism before and after birth. *The Journal of Physiology*, **601**(8), 1319–1341.

do Carmo, J. M., Omoto, A. C. M., Dai, X., Moak, S. P., Mega, G. S., Li, X., Wang, Z., Mouton, A. J., Hall, J. E., & da Silva, A. A. (2021). Sex differences in the impact of parental obesity on offspring cardiac SIRT3 expression, mitochondrial efficiency, and diastolic function early in life. *American Journal of Physiology- Heart and Circulatory Physiology*, **321**(3), H485–H495.

Duan, A. Q., Darby, J. R. T., Soo, J. Y., Lock, M. C., Zhu, M. Y., Flynn, L. V., Perumal, S. R., Macgowan, C. K., Selvanayagam, J. B., Morrison, J. L., & Seed, M. (2019). Feasibility of phase-contrast cine magnetic resonance imaging for measuring blood flow in the sheep fetus. *American Journal of Physiology- Regulatory, Integrative and Comparative Physiology*, **317**(6), R780–R792.

Farley, D., Tejero, M. E., Comuzzie, A. G., Higgins, P. B., Cox, L., Werner, S. L., Jenkins, S. L., Li, C., Choi, J., Dick, E. J., Jr., Hubbard, G. B., Frost, P., Dudley, D. J., Ballesteros, B., Wu, G., Nathanielsz, P. W., & Schlabritz-Loutsevitch, N. E. (2009). Feto-placental adaptations to maternal obesity in the baboon. *Placenta*, **30**(9), 752–760.

Forhead, A. J., & Fowden, A. L. (2014). Thyroid hormones in fetal growth and prepartum maturation. *Journal of Endocrinology*, **221**(3), R87–R103.

Guzzardi, M. A., Liistro, T., Gargani, L., Ait Ali, L., D'Angelo, G., Rocchiccioli, S., La Rosa, F., Kemeny, A., Sanguinetti, E., Ucciferri, N., De Simone, M., Bartoli, A., Festa, P., Salvadori, P. A., Burchielli, S., Sicari, R., & Iozzo, P. (2018). Maternal obesity and cardiac development in the offspring: Study in human neonates and minipigs. *Journal of the American College of Cardiology Cardiovascular Imaging*, **11**(12), 1750–1755.

Huber, H. F., Jenkins, S. L., Li, C., & Nathanielsz, P. W. (2020). Strength of nonhuman primate studies of developmental programming: review of sample sizes, challenges, and steps for future work. *Journal of Developmental Origins of Health and Disease*, **11**(3), 297–306.

Janssen, R., Muller, A., & Simonides, W. S. (2017). Cardiac thyroid hormone metabolism and heart failure. *European Thyroid Journal*, **6**(3), 130–137.

Kilkenny, C., Browne, W. J., Cuthill, I. C., Emerson, M., & Altman, D. G. (2010). Improving bioscience research reporting: The ARRIVE guidelines for reporting animal research. *PLoS Biology*, **8**(6), e1000412.

Lee, K. K., Raja, E. A., Lee, A. J., Bhattacharya, S., Bhattacharya, S., Norman, J. E., & Reynolds, R. M. (2015). Maternal obesity during pregnancy associates with premature mortality and major cardiovascular events in later life. *Hypertension*, **66**(5), 938–944.

Li, C., Jenkins, S., Considine, M. M., Cox, L. A., Gerow, K. G., Huber, H. F., & Nathanielsz, P. W. (2019). Effect of maternal obesity on fetal and postnatal baboon (Papio species) early life phenotype. *Journal of Medical Primatology*, **48**(2), 90–98.

Lie, S., Morrison, J. L., Williams-Wyss, O., Suter, C. M., Humphreys, D. T., Ozanne, S. E., Zhang, S., MacLaughlin, S. M., Kleemann, D. O., Walker, S. K., Roberts, C. T., & McMillen, I. C. (2014). Impact of embryo number and maternal undernutrition around the time of conception on insulin signaling and gluconeogenic factors and micro-RNAs in the liver of fetal sheep. *American Journal of Physiology-Endocrinology and Metabolism*, **306**(9), E1013–E1024.

Lin, Y., & Sun, Z. (2011). Thyroid hormone potentiates insulin signaling and attenuates hyperglycemia and insulin resistance in a mouse model of type 2 diabetes. *British Journal of Pharmacology*, **162**(3), 597–610.

Lock, M. C., Botting, K. J., Allison, B. J., Niu, Y., Ford, S. G., Murphy, M. P., Orgeig, S., Giussani, D. A., & Morrison, J. L. (2023). MitoQ as an antenatal antioxidant treatment improves markers of lung maturation in healthy and hypoxic pregnancy. *The Journal of Physiology*, **601**(16), 3647–3665.

Maas, A. H., & Appelman, Y. E. (2010). Gender differences in coronary heart disease. *Netherlands Heart Journal*, **18**(12), 598–602.

Maloyan, A., Muralimanoharan, S., Huffman, S., Cox, L. A., Nathanielsz, P. W., Myatt, L., & Nijland, M. J. (2013). Identification and comparative analyses of myocardial miRNAs involved in the fetal response to maternal obesity. *Physiological Genomics*, **45**(19), 889–900.

McBride, G. M., Wiese, M. D., Soo, J. Y., Darby, J. R. T., Berry, M. J., Varcoe, T. J., & Morrison, J. L. (2020). The impact of intrauterine growth restriction on cytochrome P450 enzyme expression and activity. *Placenta*, **99**, 50–62.

McGillick, E. V., Orgeig, S., McMillen, I. C., & Morrison, J. L. (2013). The fetal sheep lung does not respond to cortisol infusion during the late canalicular phase of development. *Physiological Reports*, **1**(6), e00130.

McMillen, I. C., Rattanatray, L., Duffield, J. A., Morrison, J. L., MacLaughlin, S. M., Gentili, S., & Muhlhausler, B. S. (2009). The early origins of later obesity: Pathways and mechanisms. *Advances in Experimental Medicine and Biology*, **646**, 71–81.

McMillen, I. C., & Robinson, J. S. (2005). Developmental origins of the metabolic syndrome: Prediction, plasticity, and programming. *Physiological Reviews*, **85**(2), 571–633.

Mdaki, K. S., Larsen, T. D., Wachal, A. L., Schimelpfenig, M. D., Weaver, L. J., Dooyema, S. D., Louwagie, E. J., & Baack, M. L. (2016). Maternal high-fat diet impairs cardiac function in offspring of diabetic pregnancy through metabolic stress and mitochondrial dysfunction. *American Journal of Physiology- Heart and Circulatory Physiology*, **310**(6), H681–H692.

Meakin, A. S., Nathanielsz, P. W., Li, C., Clifton, V. L., Wiese, M. D., & Morrison, J. L. (2024). Maternal obesity impacts fetal liver androgen signalling in a sex-specific manner. *Life Sciences*, **337**, 122344.

Nathanielsz, P. W., & Fisher, D. A. (1979). Thyroid function in the perinatal period. *Animal Reproduction Science*, **2**(1–3), 57–62.

Nathanielsz, P. W., Yan, J., Green, R., Nijland, M., Miller, J. W., Wu, G., McDonald, T. J., & Caudill, M. A. (2015). Maternal obesity disrupts the methionine cycle in baboon pregnancy. *Physiological Reports*, **3**(11), e12564.

Nisoli, E., Clementi, E., Carruba, M. O., & Moncada, S. (2007). Defective mitochondrial biogenesis: A hallmark of the high cardiovascular risk in the metabolic syndrome? *Circulation Research*, **100**(6), 795–806.

Pachucki, J., Hopkins, J., Peeters, R., Tu, H., Carvalho, S. D., Kaulbach, H., Abel, E. D., Wondisford, F. E., Ingwall, J. S., & Larsen, P. R. (2001). Type 2 iodothyronin deiodinase trans-gene expression in the mouse heart causes cardiac-specific thyrotoxicosis. *Endocrinology*, **142**(1), 13–20.

Pascual, F., & Coleman, R. A. (2016). Fuel availability and fate in cardiac metabolism: A tale of two substrates. *Biochimica et Biophysica Acta*, **1861**(10), 1425–1433.

Puppala, S., Li, C., Glenn, J. P., Saxena, R., Gawrieh, S., Quinn, A., Palarczyk, J., Dick, E. J., Jr., Nathanielsz, P. W., & Cox, L. A. (2018). Primate fetal hepatic responses to maternal obesity: Epigenetic signalling pathways and lipid accumulation. *The Journal of Physiology*, **596**(23), 5823–5837.

Rakhra, V., Galappaththy, S. L., Bulchandani, S., & Cabandugama, P. K. (2020). Obesity and the western diet: How we got here. *Missouri Medicine*, **117**(6), 536–538.

Randle, P. J. (1998). Regulatory interactions between lipids and carbohydrates: The glucose fatty acid cycle after 35 years. *Diabetes Metabolism Reviews*, **14**(4), 263–283.

Razaz, N., Villamor, E., Muraca, G. M., Bonamy, A. E., & Cnattingius, S. (2020). Maternal obesity and risk of cardio-vascular diseases in offspring: A population-based cohort and sibling-controlled study. *The Lancet Diabetes & Endocrinology*, **8**(7), 572–581.

Schlabritz-Loutsevitch, N. E., Howell, K., Rice, K., Glover, E. J., Nevill, C. H., Jenkins, S. L., Bill Cummins, L., Frost, P. A., McDonald, T. J., & Nathanielsz, P. W. (2004). Development of a system for individual feeding of baboons maintained in an outdoor group social environment. *Journal of Medical Primatology*, **33**(3), 117–126.

Serasinghe, M. N., & Chipuk, J. E. (2017). Mitochondrial fission in human diseases. *Handbook of Experimental Pharmacology*, **240**, 159–188.

Smith, R. L., Soeters, M. R., Wüst, R. C. I., & Houtkooper, R. H. (2018). Metabolic flexibility as an adaptation to energy resources and requirements in health and disease. *Endocrine Reviews*, **39**(4), 489–517.

Soo, P. S., Hiscock, J., Botting, K. J., Roberts, C. T., Davey, A. K., & Morrison, J. L. (2012). Maternal undernutrition reduces P-glycoprotein in guinea pig placenta and developing brain in late gestation. *Reproductive Toxicology*, **33**(3), 374–381.

Suter, M. A., Sangi-Haghpeykar, H., Showalter, L., Shope, C., Hu, M., Brown, K., Williams, S., Harris, R. A., Grove, K. L., Lane, R. H., & Aagaard, K. M. (2012). Maternal high-fat diet modulates the fetal thyroid axis and thyroid gene expression in a nonhuman primate model. *Molecular Endocrinology*, **26**(12), 2071–2080.

Tannenbaum, J., & Bennett, B. T. (2015). Russell and Burch's 3Rs then and now: The need for clarity in definition and purpose. *Journal of the American Association for Laboratory Animal Science*, **54**(2), 120–132.

Turdi, S., Ge, W., Hu, N., Bradley, K. M., Wang, X., & Ren, J. (2013). Interaction between maternal and postnatal high fat diet leads to a greater risk of myocardial dysfunction in offspring via enhanced lipotoxicity, IRS-1 serine phosphorylation and mitochondrial defects. *Journal of Molecular and Cellular Cardiology*, **55**, 117–129.

Vaughan, O. R., Rosario, F. J., Chan, J., Cox, L. A., Ferchaud-Roucher, V., Zemski-Berry, K. A., Reusch, J. E. B., Keller, A. C., Powell, T. L., & Jansson, T. (2022). Maternal obesity causes fetal cardiac hypertrophy and alters adult offspring myocardial metabolism in mice. *The Journal of Physiology*, **600**(13), 3169–3191.

Wang, J., Ma, H., Tong, C., Zhang, H., Lawlis, G. B., Li, Y., Zang, M., Ren, J., Nijland, M. J., Ford, S. P., Nathanielsz, P. W., & Li, J. (2010). Overnutrition and maternal obesity in sheep pregnancy alter the JNK-IRS-1 signaling cascades and cardiac function in the fetal heart. *Federation of American Societies for Experimental Biology Journal*, **24**(6), 2066–2076.

Wang, K. C., Lim, C. H., McMillen, I. C., Duffield, J. A., Brooks, D. A., & Morrison, J. L. (2013). Alteration of cardiac glucose metabolism in association to low birth weight: experimental evidence in lambs with left ventricular hypertrophy. *Metabolism*, **62**(11), 1662–1672.

Wang, K. C., Tosh, D. N., Zhang, S., McMillen, I. C., Duffield, J. A., Brooks, D. A., & Morrison, J. L. (2015). IGF-2R-Gαq signaling and cardiac hypertrophy in the low-birth-weight lamb. *American Journal of Physiology- Regulatory, Integrative and Comparative Physiology*, **308**(7), R627–R635.

Wang, M. C., Freaney, P. M., Perak, A. M., Greenland, P., Lloyd-Jones, D. M., Grobman, W. A., & Khan, S. S. (2021). Trends in prepregnancy obesity and association with adverse pregnancy outcomes in the United States, 2013 to 2018. *Journal of the American Heart Association*, **10**(17), e020717.

Wang, Q., Zhu, C., Sun, M., Maimaiti, R., Ford, S. P., Nathanielsz, P. W., Ren, J., & Guo, W. (2019). Maternal obesity impairs fetal cardiomyocyte contractile function in sheep. *Federation of American Societies for Experimental Biology Journal*, **33**(2), 2587–2598.

Weitzel, J. M., Iwen, K. A., & Seitz, H. J. (2003). Regulation of mitochondrial biogenesis by thyroid hormone. *Experimental Physiology*, **88**(1), 121–128.

World Health Organization (2021). Obesity and Overweight. https://www.who.int/news-room/fact-sheets/detail/obesity-and-overweight

Zambrano, E., & Nathanielsz, P. W. (2013). Mechanisms by which maternal obesity programs offspring for obesity: evidence from animal studies. *Nutrition Reviews*, **71**, (Suppl 1), S42–S54.

Zhu, M. J., Ma, Y., Long, N. M., Du, M., & Ford, S. P. (2010). Maternal obesity markedly increases placental fatty acid transporter expression and fetal blood triglycerides at midgestation in the ewe. *American Journal of Physiology-Regulatory, Integrative and Comparative Physiology*, **299**(5), R1224–R1231.

Additional information

Supporting information

Additional supporting information can be found online in the Supporting Information section at the end of the HTML view of the article. Supporting information files available:

Peer Review History